View Article Online
View Journal

RSC Advances

This article can be cited before page numbers have been issued, to do this please use: S. Radhakrishnan and S. KIM, *RSC Adv.*, 2015, DOI: 10.1039/C5RA01074H.

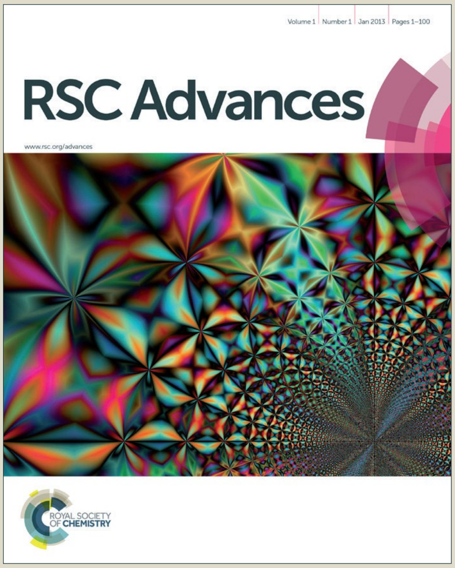
Volume 1 | Number 1 | Jan 2013 | Pages 1–100

RSC Advances

www.rsc.org/advances

ROYAL SOCIETY OF CHEMISTRY

ROYAL SOCIETY OF CHEMISTRY

www.rsc.org/advances

View Article Online
DOI: 10.1039/C5RA01074H

Facile fabrication of NiS and reduced graphene oxide hybrid film for nonenzymatic detection of glucose

Sivaprakasam Radhakrishnan, Sang Jae Kim*

Nanomaterials and System Lab, Department of Mechatronics Engineering, Jeju National University, Jeju 690-756, Republic of Korea.

***Corresponding author**

Fax number : +82 64 751 3710

Telephone : +82 64 754 3715

Email: kimsangj@jejunu.ac.kr

View Article Online
DOI: 10.1039/C5RA01074H

Abstract

In the present study, nickel sulfide (NiS) decorated reduced graphene oxide was synthesized by a facile one-step hydrothermal approach. Characterization of as-made nanohybrid using Field emission scanning electron microscope (FE-SEM) and powder X-ray diffraction (XRD) clearly demonstrate the successful attachment of NiS onto the rGO nanosheets. Further, the prepared NiS-rGO nanohybrid has been examined for the electrochemical nonenzymatic detection of glucose using cyclic voltammetry, linear sweep voltammetry and amperometry. The electrochemical studies demonstrated that NiS-rGO nanohybrid modified electrode detects glucose linearly over a concentration range of 5.0×10^{-5} – 1.7×10^{-3} M with a detection limit of 1.0×10^{-5} M. The obtained detection limit for NiS-rGO nanohybrid is very much comparable to the recent literature values. Further, the NiS-rGO nanohybrid modified electrode showed an excellent anti-interference ability against electroactive species and showed good reproducibility and stability.

Keywords: *Reduced graphene oxide, nickel sulfide, glucose, electrochemical, biosensors*

View Article Online
DOI: 10.1039/C5RA01074H

1 Introduction

Development of glucose sensor is of great importance in a many fields including clinical diagnostics, biotechnology, environmental monitoring, pharmaceutical analysis and food industries [1,2]. Up to now, several methods such as fluorescence, optical, acoustic, surface plasmon resonance, electro-chemiluminescence, and electrochemical have been established for the determination of glucose [3-6]. Compared with these methods, electrochemical approach have become a considerably interesting approach due to its many merits such as compact, relatively inexpensive, reliable, sensitive and real-time analysis. Most of the electrochemical detection of glucose is based on the enzymatic reaction [7]. However, the serious drawback is the instability of the enzyme activity, due to factors such as temperature, pH, toxic chemicals and oxygen, restricts the use of enzyme-based biosensor [8]. In addition, the attachment and stabilization protocol of the enzyme is very complicated. Considering these problems, many efforts have been tried for the electrochemical determination of glucose without using enzyme based on metal nanoparticle, metal oxide, carbon nanostructure or composites of these [9,10].

Carbon nanostructure (fullerenes, carbon nanotubes and reduced graphene oxide) has been widely used in electrocatalysis due to their low cost, wide potential window, small residual current, easy renewable surface and relatively inert electrochemistry in both aqueous and non-aqueous media. It is well known that graphene, a perfect two-dimensional (2D) material, has been extensively used for growing and anchoring of meal sulfides (CoS, NiS and CuS etc) due to their unique physical and chemical properties. In this decade, metal sulfide/graphene composite materials (Graphene- CoS, NiS-graphene and CuS-graphene etc) have attracted a great deal of attention due to their improved electrocatalytic properties [11-13].

View Article Online
DOI: 10.1039/C5RA01074H

Metal sulfide nanostructures with large surface area offer particular advantages to electrocatalytic performance due to their large specific surface area and easy transport of analyte.

Nickel sulfide (NiS), one member of the important metal sulfides, has been extensively used for electrocatalyst [14], supercapcitors [15], lithium ion batteries [16], dye-sensitized solar cells [17] etc. due to their high electronic conduction, low cost, easy of production and storage. In general, Ni-based nanostructured materials have shown excellent electrocatalytic properties towards glucose detection. Ni-based nanomaterials have been employed for glucose detection using the reduction/oxidation reaction of $Ni(OH)_2$/NiOOH. Several approaches have been used to synthesis metal sulfide nanostructures; liquid-phase synthesis and hot-injection etc. Further, these methods are obviously involving complicated experimental set-up with high energy consuming and expensive instrumentation techniques. Therefore, simple nickel sulfide preparation and electrode modification protocol with improved sensing performance of glucose is highly required.

Here, we report the synthesis of NiS-rGO nanohybrid by a one-pot facile hydrothermal method and its application for the nonenzymatic detection of glucose. To our best known, NiS-reduced graphene oxide nanohybrid have never been reported and systematically studied to be used for nonenzymatic glucose detection. The performance of the newly fabricated glucose biosensor was studied using cyclic voltammetry (CV), electrochemical impedance spectroscopy (EIS) and amperometry and the results are discussed. The fabricated sensor showed high sensitivity, stability and satisfactory reproducibility.

View Article Online
DOI: 10.1039/C5RA01074H

2 Experimental

2.1 *Materials*

Nickel sulfate, thiourea, isopropoanol, glucose and ammonia are purchased from Daejung Chemicals Ltd, South Korea. The phosphate buffer solutions with different pH values were prepared using Na_2HPO_4 and NaH_2PO_4. All the reagents were of analytical grade and used without further purification.

2.2 *Instrumentation*

The surface morphologies of the nanohybrid were characterized using a field emission-scanning electron microscope (FE-SEM) JEOL JSM-6700F. The phase purity and crystalline nature of the prepared materials were studied using the powder X-ray diffraction technique (XRD, Rigaku, Cu Kα radiation operating at 40 KeV/40 mA). Electrochemical measurements were performed in a conventional two compartment three electrode cell with a mirror polished 3 mm glassy carbon (GC) as the working electrode, Pt wire as the counter electrode and an Ag/AgCl (3M KCl) as the reference electrode. The electrochemical measurements were carried out with an AUTOLAB (Model PGSTAT302N, Netherlands). All electrochemical measurements were carried out in a nitrogen saturated 0.1 M NaOH solution for 15 min. Cyclic voltammograms were recorded between a potential window of - 0.2 V and 0.6 V at a scan rate of 50 mVs^{-1} in 0.1 M KCl solution containing 1.0 mM $[Fe(CN)_6]^{3-/4-}$ redox couple. The electrochemical impedance spectroscopy (EIS) measurements were carried out by applying an ac potential of amplitude 10 mV over the dc potential of 200 mV in the frequency range of 100 KHz to 1 Hz. The impedance data are presented in the form of Nyquist plots. The value of the charge transfer resistance (R_{ct}) was determined using Zsimpwin software simulations.

View Article Online
DOI: 10.1039/C5RA01074H

2.3 Preparation of NiS-rGO nanohybrid

Graphene oxide (GO) was synthesized from natural graphite powders by a modified Hummers method as described in our earlier report [18]. The NiS-rGO nanohybrid was prepared by a hydrothermal method. Briefly, 50 mg graphene oxide was dispersed in 70 mL (1:1) solution of isopropanol and double distilled water followed by ultrasonicated for 30 min. Then, 5mM $NiSO_4$, 15 mM thiourea and 25 % ammonia (10 mL) were added into the solution. Afterwards, the mixture was sealed into a Teflon-lined stainless steel autoclave and maintained at 170 °C for 20 h and then cooled to room temperature gradually. Subsequently, the precipitation was filtered, washed with distilled water and ethanol several times, and dried at 80 °C for 6 h in a vacuum oven. For comparison, pure NiS and reduced graphene oxide (rGO) were prepared by the same method.

2.4 NiS-rGO nanohybrid modified electrode

The NiS-rGO nanohybrid modified the glassy carbon (GC) electrode was prepared as follows. First, the surface of the GC electrode for each experiment was mechanically polished with alumina suspensions (0.5 and 1.0 µM respectively). After that, the electrode was successively washed in ethanol and water for 2 min. by ultrasonic method. A 10 µL aliquot of NiS-rGO hybrid (dispersion in water, 0.5 mg mL^{-1}) was dropped onto the surface of GC electrode and dried under room temperature (Scheme 1). In addition, rGO and NiS modified GC electrodes were prepared by the above mentioned process for comparison.

<Scheme 1>

View Article Online
DOI: 10.1039/C5RA01074H

3 Results and Discussion

3.1 Characterization of the as-prepared NiS-rGO hybrids

The microstructure and morphology of the NiS and NiS-rGO were characterized by FE-SEM. Fig. 1 shows the FE-SEM micrographs of the NiS (A) and NiS-rGO (B). Fig. 1A shows the urchin like NiS exhibiting a diameter between 70-120 nm. Fig.1B shows the NiS-rGO nanohybrid, it can be seen that the NiS was well decorated on the reduced graphene oxide sheets. These results clearly indicate the presence of strong interaction between NiS and rGO. The presence of micro urchin NiS on high surface area of reduced graphene oxide nanosheet hybrid may create a better communication between the electrode surface and sensing analyte. This was confirmed by the XRD for NiS-rGO hybrids shown in Fig.1C, together with bare NiS (curve a). The diffraction patterns of the NiS-rGO hybrid (curve b) corresponding to pure phases of NiS (JCPDS file number 86-2281). All the peaks observed in the NiS-rGO hybrids are related to the NiS (as shown in Fig. 1C).

The possible reaction mechanism of the micro urchin NiS formation is tentatively proposed as follow as.

$$S{=}C(NH_2)_2 + 2H_2O \rightarrow H_2S + 2NH_3 + CO_2 \quad (1)$$

$$Ni^{2+} + 4NH_3 \rightarrow [Ni(NH_3)_4]^{2+} \quad (2)$$

$$NH_3 + H_2O \rightarrow OH^- + NH_4^+ \quad (3)$$

$$H_2S + 2OH^- \rightarrow S^{2-} + 2H_2O \quad (4)$$

$$[Ni(NH_3)_4]^{2+} + S^{2-} \rightarrow NiS + 4NH_3 \quad (5)$$

<Fig. 1>

3.2 CV and EIS studies on NiS-rGO modified GC electrode

The cyclic voltammogram (CV) curves of the bare GC (curve a), NiS (curve b) and NiS-rGO (curve c) modified electrodes recorded in the presence of 1mM $[Fe(CN)_6]^{3-/4-}$ in 0.1 M KCl at a scan rate 50 mVs^{-1} are shown in Fig. 2A. At the bare GC electrode (curve a), a pair of well defined redox peak was observed (I_{pa} : 19.5 µA and E_{pa}/E_{pc} : 0.237/0.163) for Fe(III)/Fe(II) redox reaction. In contrast, two pairs of well distinguished redox peaks with increasing peak current and decreasing peak to peak separation values (I_{pa} : 21.5 µA and E_{pa}/E_{pc} 0.239/0.161) for Fe(III)/Fe(II) and (I_{pa} : 69.7µA and E_{pa}/E_{pc} 0.616/0.565) for Ni(III)/Ni(II) were obtained for NiS-rGO (curve c) modified GC electrode when compared to pure NiS (curve b) modified GC electrode (I_{pa} : 15 µA and E_{pa}/E_{pc} 0.291/0.125) for Fe(III)/Fe(II) and (I_{pa} : 9.02 µA and $\mathrm{E_{pa}/E_{pc}}$ 0.591/0.567) for Ni(III)/Ni(II) redox reaction. This could be attributed to the sheet like structure with high surface area and good electrical conductivity of the NiS-rGO hybrid which allow the diffusion of more $[Fe(CN)_6]^{3-/4-}$ redox couple on its surface. Further, the catalytic properties of NiS were grafted onto the rGO sheets which is highly active than that of pure NiS and also restrict the formation of face-to-face stacking in rGO sheets. The experimental results are consistent with the reported literature [19,20]. These results clearly indicate that the newly formed NiS-rGO hybrid have newer functionalities which are different from those of single (alone rGO and NiS) component nano materials.

Fig. 2B shows the Nyquist diagrams obtained using electrochemical impedance spectroscopy for bare GC, NiS and NiS-rGO modified GC electrodes. The charge transport process of the modified electrodes was studied by monitoring charge transfer resistance (R_{CT}) at the electrode/electrolyte interface. The Nyquist diagrams were fit by Randels equivalent circuit shown in Fig. 2C, which includes the following electronic elements: R_s is the solution resistance,

View Article Online
DOI: 10.1039/C5RA01074H

R_{CT} is the charge transfer resistance, W is the Warburg impedance and Q_{CPE} is the constant phase element (CPE). The value of the charge transfer resistance (R_{CT}) for the bare GC (curve a), NiS (curve b) and NiS-rGO (curve c) modified GC electrodes were estimated to be 157, 2542 and 76 Ω cm^2, respectively. These results are in good agreement with the peak current (i_{pa}) values obtained from CVs measurements. Hence we have used NiS-rGO modified GC electrode for further investigation.

The electrochemical behavior of NiS-rGO modified electrode was further investigated in 0.1 M KCl solution containing 1mM $[\mathrm{Fe(CN)_6}]^{3-/4-}$ as a redox probe. Fig. 2D shows various cyclic voltammograms recorded at different scan rates (10-100 mVs^{-1}) for NiS-rGO modified GC electrode. It can be seen that the anodic and cathodic peak current increases with increasing scan rates (10-100 mVs^{-1}). Further, a good linearity was obtained while plotting the current against square root of scan rate (inset of Fig. 2D), indicating that the oxidation of $[\mathrm{Fe(CN)_6}]^{3-/4-}$ was diffusion controlled process.

< Fig.2 >

3.3 Electrochemical determination of glucose

To investigate electrochemical determination of glucose, we have carried out cyclic voltammetry of the NiS-rGO modified GC electrode in 0.1 M NaOH solution with and without 5.0×10^{-4} M glucose. As shown in Fig.3A the anodic peak current (I_{pa}) was greatly improved from 138 µA to 175 µA when the NiS-rGO modified electrode was exposed to glucose solution. It is also noted that the oxidation peak current was higher and the cathodic peak current was lower in the presence of glucose than in the absence of glucose. It is clearly indicates that NiS-

View Article Online
DOI: 10.1039/C5RA01074H

rGO has good electrocatalyst towards the direct oxidation of glucose, consistent with earlier reports [21,22].

In blank NaOH solution, the NiS-rGO modified electrode showed a pair of well redox peaks and these are assigned to the Ni(II)/Ni(III) redox couple in alkaline medium (Fig. S1). Further, both the anodic and cathodic peak currents were linearly proportional to the square root of the scan rate indicated that the electrochemical process was typically diffusion-controlled process (Fig. S2). In addition, the bare GC electrode did not show any oxidation response in the presence of glucose (Fig. S3). The catalytic mechanism of the NiS-rGO to glucose oxidation can be simply explained as follow as.

$$\mathrm{NiS} + \mathrm{OH}^- \rightarrow \mathrm{NiSOH} + e^- \qquad (6)$$

$$\mathrm{NiSOH} + \text{glucose} \rightarrow \mathrm{NiS} + \text{glucolactone} \qquad (7)$$

Further, the effect of scan rate on the electrocatalytic oxidation of 5.0×10^{-4} M glucose at the NiS-rGO modified GC electrode was investigated by CV. Both the oxidation and reduction peak currents increased gradually with the increase of scan rates (v) (50-150 $\mathrm{mVs^{-1}}$) in 0.1 M NaOH solution are shown in Fig. 3B. A good linearity was obtained while plotting the current against square root of scan rate with a correlation coefficient of 0.9993 (inset of Fig. 3B), indicating that the oxidation of glucose was diffusion controlled process [23].

Fig. 3C shows the linear sweep voltammograms (LSVs) obtained for glucose in the concentration range of 0-1000 μM at the NiS-rGO modified GC electrode. The oxidation current of glucose increased with a slight positive potential shift in the oxidation peak potential upon each increment of 100 μM. The oxidation currents had a linear relationship with the concentration of glucose with a correlation coefficient of 0.9991 (inset of Fig.3C).

View Article Online
DOI: 10.1039/C5RA01074H

< Fig.3 >

Furthermore, the amperometric experiment was investigated for the NiS-rGO modified GC electrode towards the detection of glucose. Fig. 4A shows the amperometric *i-t* curve for glucose at the NiS-rGO modified electrode in a homogeneously stirred 0.1 M NaOH solution at an applied potential of + 0.5 V. The modified electrode showed an initial response due to 5.0×10^{-5} M glucose and on adding the different amount of glucose in each step with a sample interval of 50 s, the current response linearly increased, and a steady state current response was attained within 2 s. The amperometric current linearly increased when the concentration of glucose was increased from $5.0 \times 10^{-5} - 1.7 \times 10^{-3}$ M at the NiS-rGO modified GC electrode with a correlation coefficient of 0.9995. The detection limit was found to be 1.0×10^{-5} M. This value is very much comparable to the literature reports (supplementary Table 1).

Selectivity is one of the most important parameters of a biosensor. In particular, it is very essential to apply for nonenzymatic glucose biosensor. We have demonstrated the selective determination of 0.1 mM glucose in the presence of 0.05mM physiological interfering compounds such as lactose, riboflavin, ascorbic acid, dopamine and uric acid based on NiS-rGO modified GC electrode in 0.5 M NaOH at an applied potential of 0.5 V. As shown in Fig.4B, the interference currents by lactose, riboflavin, ascorbic acid, dopamine and uric acid were negligible, unlike the strong response by glucose. The normalized peak current response *vs*. interference compounds was given as bar diagram (inset of Fig. 4B). These results suggest that the NiS-rGO modified GC electrode was highly selective towards glucose from the aforementioned interfering compounds.

View Article Online
DOI: 10.1039/C5RA01074H

To ascertain the reproducibility of the results, four different GC electrodes were modified with NiS-rGO hybrid and their amperometric response towards the oxidation of 0.10 mM glucose was tested. The peak current obtained in the measurements of three independent electrodes showed a relative standard deviation of 4.23 %, confirming that the results are reproducible. The storage stability of our fabricated NiS-rGO electrode was examined by amperometric current responses to 0.10 mM glucose after 15 and 30 days of storage in air under room temperature. The current response decreased about 2.1 % in 15 days and 3.0 % in about 30 days. There is no much significant change in the amperometric current response for glucose detection. These results indicate that the NiS-rGO modified electrode has a good reproducibility and stability.

The main advantages of the newly fabricated glucose sensor is that the NiS-rGO nanohybrid preparation (eco-friendly hydrothermal approach) and electrode modification (simple drop casting) procedure adopted in the present study is very simple when compared to the literature reports. The performance of the fabricated glucose sensor is very much comparable to the literature values. The superiority of the present sensor can be attributed to the fact that the synergistic effects from the combination between the good electrocatalyst of NiS and an effective large surface with high electrical conductivity of rGO in the nanoscale.

<Fig. 4>

4. Conclusion

We have successfully synthesized NiS-rGO nanohybrid by an environment-friendly approach and their demonstrated that the NiS-rGO nanohybrid modified electrode offers a good, reliable and simple method for nonenzymatic detection of glucose. The NiS-rGO modified

View Article Online
DOI: 10.1039/C5RA01074H

electrode provided a sheet like structure with large effective surface area, which could act as electron transfer medium and promote the charge transfer between electrode surface and glucose. The amperometric current increased linearly while increasing the concentration of glucose from $5.0 \times 10^{-5} – 1.7 \times 10^{-3}$ M with lowest detection limit of 1.0×10^{-5} M. Excellent performance in sensitivity, stability, reproducibility and selectivity was achieved when the sensor was exposed to glucose solution. All these advantageous features can make the proposed sensor applicable in health care, food industries and other areas.

Acknowledgement

This research was supported by Basic Science Research Program through the National Research Foundation of Korea (NRF) funded by the Ministry of Science, ICT & Future Planning (2013R1A2A2A01068926)

View Article Online
DOI: 10.1039/C5RA01074H

References

1. L. Torsi, A. Dodabalapour, *Anal. Chem.*, 2005, **77**, 380A-387A.
2. J. Gonzalo-Ruiz, M.A. Alonso-Lomillo, F.J. Munoz, *Biosens. Bioelectron.*, 2007, **22** 1517-1521.
3. J. Wang, *Chem. Rev.*, 2008, **108**, 814-825.
4. V. Scognamigli, *Biosens. Bioelectron.*, 2013, **47**, 12-25.
5. A. Heller, B. Feldman, *Chem. Rev.*, 2008, **108**, 2482-2505.
6. N.J. Ronkainen, H.B. Halsall, W.R. Heineman, *Chem. Soc. Rev.*, 2010, **39**, 1747-1763.
7. J. Wu, F. Yin, *J. Electroanal. Chem.*, 2013, **694**, 1-5.
8. S. Park, H. Boo, T.D. Chung, *Anal. Chem. Acta*, 2000, **556**, 46-57.
9. K. Tian, M. Prestgard, A. Tiwari, *Mater. Sci. Eng*. 2014, **41**, 100-118.
10. S. Peng, Y. Huang, T. Wang, J. Ma, *RSC Adv*., 2013, **3**, 3487-3502.
11. G. Yan, Y. Xu, Y. Wang, ACS. Appl. *Mater. Interfaces*, 2013, **5**, 801-806.
12. H. Bi, W. Zhao, S. Sun, H. Cui, T. Lin, F. Huang, X. Xie, M. Jiang, *Carbon*, 2013, **61** 116-123.
13. H-C. Tao, X-L. Yang, L-L. Zhang, S-B. Ni, *J. Phys. Chem. Solids*, 2014, **75**, 1205-1209.
14. T-W. Lin, C-J. Liu, C-S. Dai, *Appl. Catal. B*, 2014, **154-155**, 213-220.
15. T. Zhu, H.B. Wu, Y. Wang, R. Xu, X.W. Lou, *Adv. Energy Mater*., 2012, **2**, 1497-1502.
16. Y. Wang, Q. Zhu, L. Tao, X. Su, *J. Mater. Chem*., 2011, **21**, 9248-9254.
17. Z. Ku, X. Li, G. Liu, H. Wang, Y. Rong, M. Xu, L. Liu, M. Hu, Y. Yang, H. Han, *J. Mat. Chem*. A 2013, **1**, 237-240.
18. S. Radhakrishnan, K. Karthikeyan, C. Sekar, J. Wilson, S.J. Kim, *Appl. Catal*. B, 2014, **148-149**, 22-28.

View Article Online
DOI: 10.1039/C5RA01074H

19. L.M. Lu, L. Zhang, F.L. Qu, H.X. Lu, X.B. Zhang, Z.S. Wu, S.Y. Huan, Q.A. Wang, G.L. Shen, R.Q. Yu, *Biosens. Bioelectron*., 2009, **25**, 218-223.
20. Y. Mu, D.L. Jia, Y.Y. He, Y.Q. Miao, H.L. Wu, *Biosens. Bioelectron*., 2011, **26**, 2948-2952.
21. H. Nie, Z. Yao, X. Zhou, Z. Yang, S. Huang, *Biosens. Bioelectron*., 2011, **30**, 28-34.
22. M. Shamsipur, M. Najafi, M.R.M. Hosseini, *Bioelectrochem*., 2010, **77**, 120-124.
23. M-M. Guo, X-L. Yin, C-H. Zhou, Y. Xia, W. Huang, Z. Li, *Electrochim. Acta*, 2014, **142**, 351-358.
24. M.C.D. Cooray, Y. Liu, S.J. Langford, A.M. Bond, J. Zhang, *Anal. Chim. Acta*, 2015, **856**, 27-34.
25. Q. Sheng, H. Mei, H. Wu, X. Zhang, S. Wang, , Sensor Actuat. B-Chem. B, 2015, **207**, 51-58.

View Article Online
DOI: 10.1039/C5RA01074H

Figure Captions

Fig. 1 SEM images of (A) NiS, (B) NiS-rGO and (C) XRD spectra of NiS and Nis-rGO.

Fig. 2 (A) CV behavior of the modified GC electrodes in presence of 1mM $[Fe(CN)_6]^{3-/4-}$ in 0.1 M KCl at a scan rate of 50 mV/s. (B) EIS behavior of the modified GC electrodes measured by impedance in the frequency region from 100 KHz to 0.1 Hz at a DC potential of 200 mV and AC potential of ± 10 mV in presence of 1mM $[Fe(CN)_6]^{3-/4-}$ in 0.1 M KCl. Curve a : bare GC, curve b : NiS and curve C : NiS-rGO modified electrodes. (C) The equivalent circuit used for fitting the impedance data. (D) CV recorded at 10-100 mV/s for NiS-rGO modified GC electrode in presence of 1mM $[Fe(CN)_6]^{3-/4-}$ in 0.1 M KCl.

Fig. 3 (A) Cyclic voltammograms of NiS-rGO modified GC electrode with (curve b) and wothout (curve a) the presence of 5.0×10^{-4} M in 0.1 M NaOH solution at a scan rate of 50 mV/s. (B) Cyclic voltammograms of NiS-rGO modified electrode at scan rates of 50 to 150 mV/s in 0.1 M NaOH solution containing 5.0×10^{-4} M; Inset shows the resulting calibration plot. (C) LSVs obtained for glucose in the cocnetrations ranging from 0 to 1000 µM. Glucose was added in steps of 100 µM each at the NiS-rGO modified electrode in 0.1 M NaOH.

Fig. 4 (A) Amperometic response of the NiS-rGO modified electrode in 0.1 M NaOH with various concentrations of glucose ($5.0 \times 10^{-5} - 1.7 \times 10^{-3}$ M). Inset shows the resulting calibration plot. (B) Amperometric response for the addition of 0.1 mM glucose curves (a) and 0.05 mM of lactose, riboflavin, ascorbic acid, dopamine and uric acid curves (b-f) and final addition of 0.1 mM of glucose (g) at NiS-rGO modified electrode in 0.1 M

View Article Online
DOI: 10.1039/C5RA01074H

NaOH. Inset shows the bar diagram of normalized amprometric current against interference compounds.

Scheme 1 Glucose detection scheme using NiS-rGO modified glassy carbon electrode.

View Article Online
DOI: 10.1039/C5RA01074H

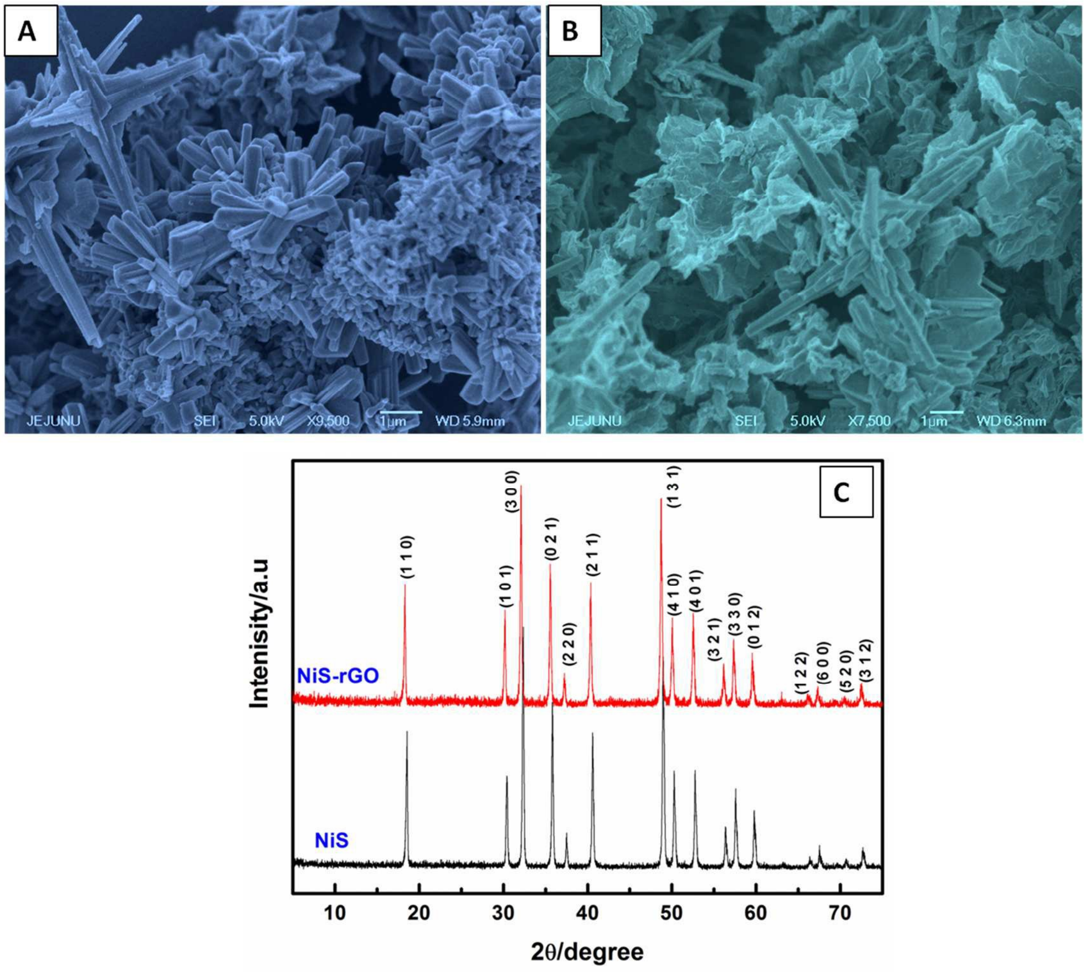

Fig. 1

View Article Online
DOI: 10.1039/C5RA01074H

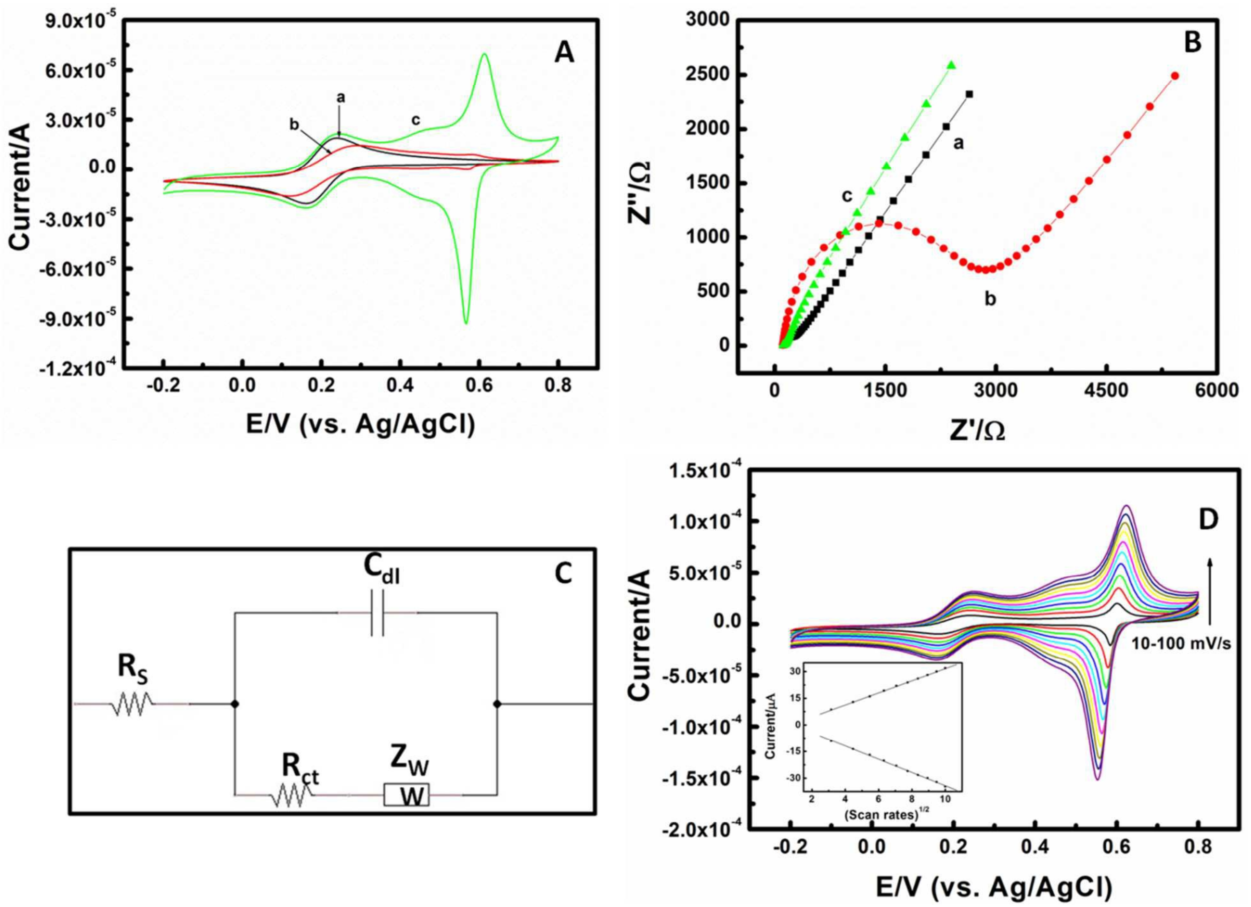

Fig. 2

View Article Online
DOI: 10.1039/C5RA01074H

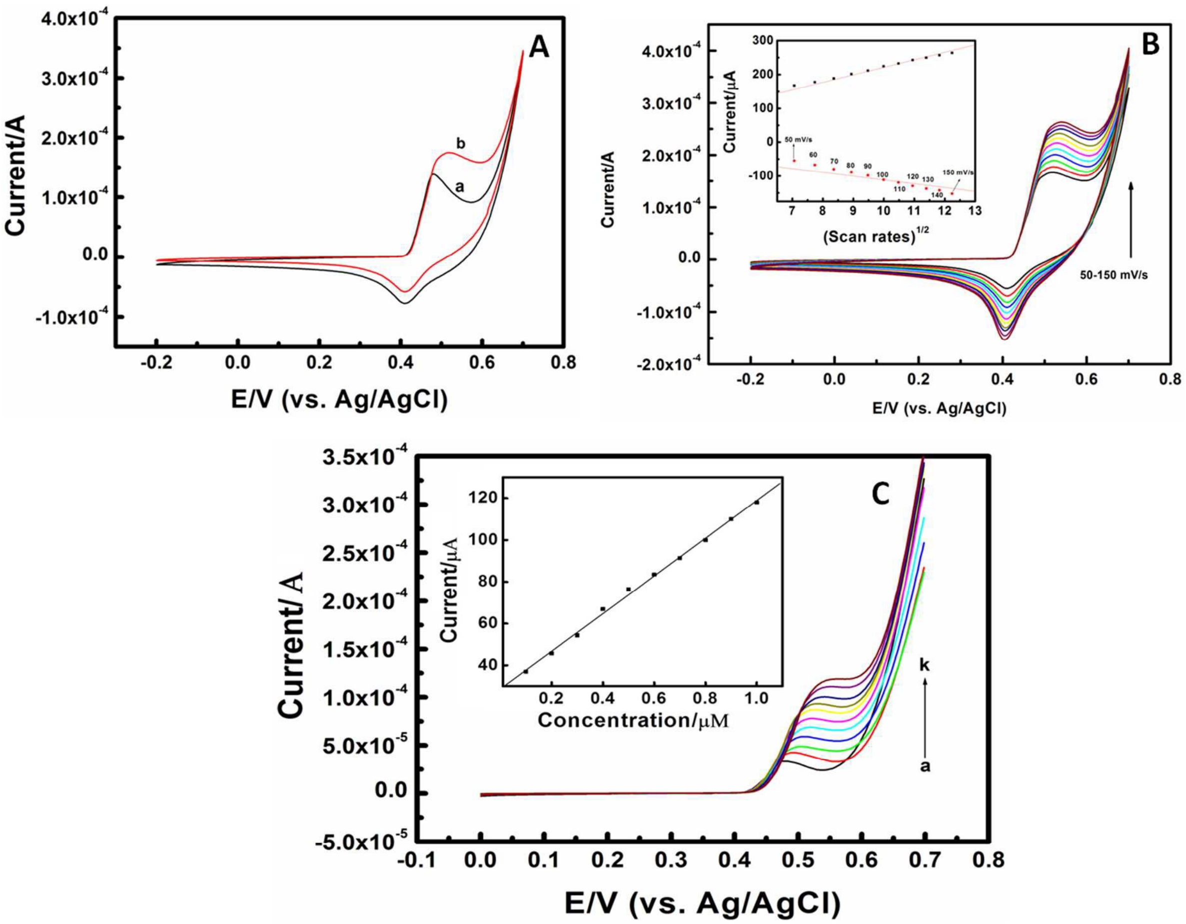

Fig. 3

View Article Online
DOI: 10.1039/C5RA01074H

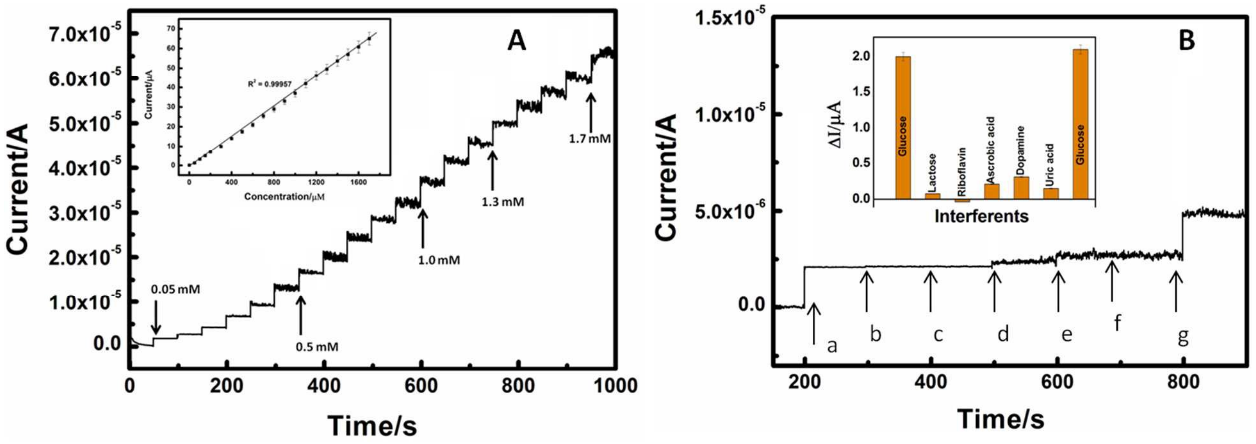

Fig. 4

View Article Online
DOI: 10.1039/C5RA01074H

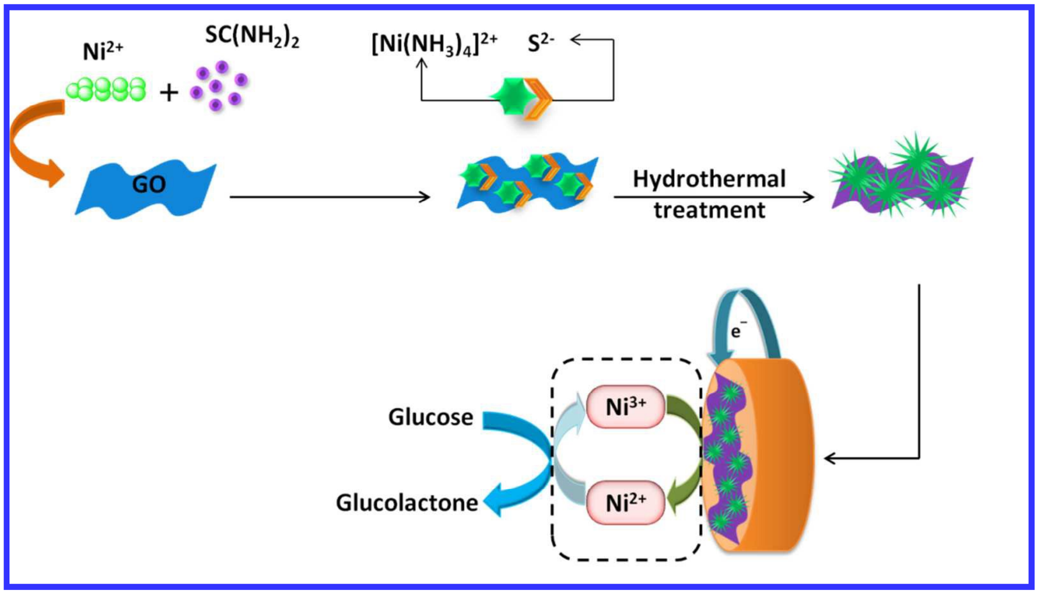

Scheme-1

View Article Online
DOI: 10.1039/C5RA01074H

Graphical Abstract